XVI International Conference on Durability of Building Materials and Components
DBMC 2023, China
K.F. Li and D.P. Fang (Eds)

Corrosion Mechanisms of Reinforced Alkali-Activated Concrete

Feng Zhang[1], **Shangtong Yang**[1]

[1]Department of Civil and Environmental Engineering, University of Strathclyde, Glasgow, G1 1XJ, UK, feng.zhang@strath.ac.uk (Feng Zhang), shangtong.yang@strath.ac.uk (Shangtong Yang)

Abstract. *Alkali-activated concrete (AAC), which exhibits good mechanical strength and chemical resistance properties, has attracted emerging interest from the research perspective considering the sustainable development of construction materials. However, the corrosion mechanism at the steel-AAC interface is not yet well understood including the physical and chemical aspects, which leads to different accumulation and evaluation of corrosion products, compared to ordinary Portland cement (OPC) concrete. In this paper, concrete pull-out test and electrochemical techniques were used to investigate the bond-slip behaviour and the evolution of deterioration of AAC respectively. In addition, the current guidance of corrosion evaluation used for OPC concrete based on ASTM C876 is not suitable for AAC. Five mixed ratios of blended fly ash and slag AAC were investigated under two chloride environments and one non-chloride environment, i.e., (1) 3.5% NaCl salt fog spray in the environmental chamber; (2) 3.5% NaCl saltwater immersion; (3) tap water immersion. Electrochemical techniques include half-cell potential, linear polarization resistance and Tafel extrapolation method were used to determine the corrosion rate. The electrochemical results are validated through the comparison of the gravimetric loss of steel after corrosion and electrochemical loss from calculation.*

Keywords: *Alkali-activated concrete, Electrochemical techniques, Sustainable development, Corrosion evolution, Electrochemical measurement.*

1 Introduction

Alkali-activated materials (AAMs) are a type of cementitious material that is activated by a high-concentration alkaline solution, such as sodium hydroxide solution. These materials are generally manufactured using industrial wastes or by-products, e.g., fly ash, produced from coal combustion in thermal power plants. AAMs are recognized as an environmentally friendly and sustainable alternative cementitious material to ordinary Portland cement due to less greenhouse gas (CO_2) emissions and reduced energy consumption regarding the manufacturing process (Ali et al., 2011).

Chloride ingress-induced reinforced concrete corrosion, e.g., using de-icing salt on the bridge deck, is a severe problem that causes permanent deterioration of concrete structures, which decreases their service life. Alkali-activated concrete (AAC) was reported to have better or comparable chloride resistance than ordinary Portland cement (OPC) concrete (Bouteiller et al., 2012, Kupwade-Patil and Allouche, 2013). Meanwhile, AAC was also reported to have a similar or better bond strength than OPC concrete (Sarker, 2011, Castel and Foster, 2015), which is attributed to the denser and more compact interfacial zone in AAC (Shi et al., 2018). However, the corrosion mechanism at the steel-AAC interface over the long term remains unclear. Since there has been limited research conducted in this area, it is important to investigate the long-term bond strength of AAC before using AAC in practice.

Non-destructive technology using electrochemical measurement means, which involves half-cell potential, linear polarization resistance (LPR), Tafel extrapolation method, and electrochemical impedance spectroscopy (EIS), is very commonly used to detect the corrosion

of concrete structures. In recent decades, it has been reported that the corrosion assessment criteria for OPC concrete is not suitable for the AAC. One reason is due to the presence of sulphide in precursors, which causes a more negative half-cell potential value that could be up to -600 mV at early age of AAC. In addition, the empirical value of Tafel constant B that is used to calculate the corrosion rate, i.e., 26 mV for the active sample and 52 mV for the passive sample, has been reported insensible (Babaee and Castel, 2016) to AAC. New experimental data thus are urgently needed to avoid any inaccurate determination of the corrosion rate of reinforced AAC.

In this study, the blended fly ash and slag AAC samples were cast to study the electrochemical behaviour and bond performance of AAC incorporated with electrochemical techniques including half-cell potential, LPR, and Tafel extrapolation method and pull-out test. A total of 90 electrochemical samples with different mix proportions and 20 pull-out samples were cast and prepared. Two artificial corrosion environments cyclic wetting/drying and saltwater immersion, and one control environment where tap water immersion has been used. The results to be obtained will advise the suitability of existing criteria used to assess corrosion likelihood in AAC.

2 Experiment Program

2.1 AAC Mixed Design and Precursors

Two types of alkali-activated materials, which are Class F fly ash (FA, according to ASTM C618) from Tarmac, UK, and ground granulated blast furnace slag (GGBS, it is also named SA in this report) supplied by Hanson cement, UK, are used to investigate the corrosion behaviour of steel-reinforced AAC. The major chemical compositions of these two materials determined by X-ray fluorescence (XRF) analysis are listed in Table 1.

Table 1. Chemical compositions of FA and GGBS determined by XRF analysis.

Chemical compositions	Class F fly ash [wt.%]	GGBS [wt.%]
SiO_2	53.22	35.90
AL_2O_3	20.48	14.20
Fe_2O_3	8.03	0.99
CaO	6.64	41.13
MgO	1.81	6.66
SO_3	1.60	0.13
Loss on Ignition (L.O.I)	3.21	1.38

A mixture of sodium hydroxide (NaOH) solution and sodium silicate (Na_2SiO_3) solution was used as the alkaline activators for AAC. The sodium hydroxide solution was prepared by dissolving the NaOH pellets that were at least 98% pure in water, which were supplied by Fisher Scientific, UK. The concentration of sodium hydroxide solution used was 12 M which consisted of 480 g pellets per litre. The prepared sodium hydroxide solution was cooled down to room temperature before using it. The sodium silicate solution from Fisher Scientific, UK, has a chemical composition that contains 13.5% Na_2O, 26.5% SiO_2, and 60% H_2O by mass. The mixed ratio of sodium silicate solution to sodium hydroxide solution used was 2.5 (by mass)

which aims to achieve maximum strength and suitable workability. Besides, the 1.5% (by mass of precursors) ADVA XR 3090 superplasticizer was used to decrease the amount water that was being used.

The mixed proportion of AAC specimens is shown in Table 2. Five groups covering two microstructure systems (N-A-S-H & C-A-S-H) of AAC were designed. After casting, the moulds were sealed with plastic film to prevent evaporation of pore moisture. The samples were then transferred to the oven for heat curing at 60 ℃ for 24 h. This process aims to gain early mechanical strength because the strength of AAC grows slowly in nature when blended with fly ash (Ismail et al., 2014). Then, specimens were de-moulded after heat curing and cured in the lab environment (20 ℃, 40% RH) until the test date. Nine 100 mm standard cubes, group 3 from Table 2, were cast to test the compressive strength at 7 days, 14 days, and 28 days, which the average compressive strength is 55.83 MPa, 60.78 MPa, and 63.08 MPa respectively.

Table 2. The mixed proportion for alkali-activated concrete (Unit: kg/m^3).

Materials	Group 1	Group 2	Group 3	Group 4	Group 5
GGBS	400	280	200	120	0
Fly ash	0	120	200	200	400
NaOH solution	44.06				
Na_2SiO_3 solution	110.15				
Sand	640				
Coarse aggregate	1152				
Free water	43.09				
Superplasticizer	6				

2.2 Electrochemical Measurement

Specimens among five groups of Table 2 were cast for the electrochemical measurement, and the design configuration of the specimen is shown in Figure 1. It is a 40 mm x 40 mm x 80 mm prism with Ø6 mm rebar in the middle. To initiate corrosion at the specific area on the steel surface, the heat shrink tube is used to coat the rebar and silicone is used to seal the sides after the tube has shrunk. A copper wire is wrapped on one side of exposed rebar. Then, both sides of the exposed rebar are covered with acrylic tube and sealed with epoxy resin.

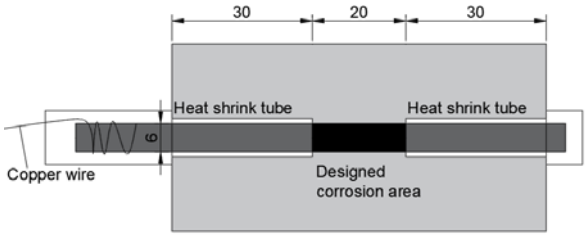

Figure 1. Design configuration of AAC specimen for electrochemical measurement (unit: mm).

The electrochemical parameters involving half-cell potential (E_{ocp}), linear polarization resistance (LPR) R_P, and the Tafel slope (β_a, β_c) and Tafel constant B will be measured before and after the corrosion test begins. To do this, the electrochemical workstation with the three-

electrode system is used, as shown in Figure 2. The steel rebar in concrete works as the working electrode (WE) along with a suitable reference electrode (RE), a saturated calomel electrode (SCE), and a counter electrode (CE) like a titanium mesh that forms the electric circuit with WE. The half-cell potential (E_{ocp}) was determined by the potential difference between the WE and RE. The stability of the entire system was guaranteed while the deviation of E_{ocp} is lower than 2 mV/min.

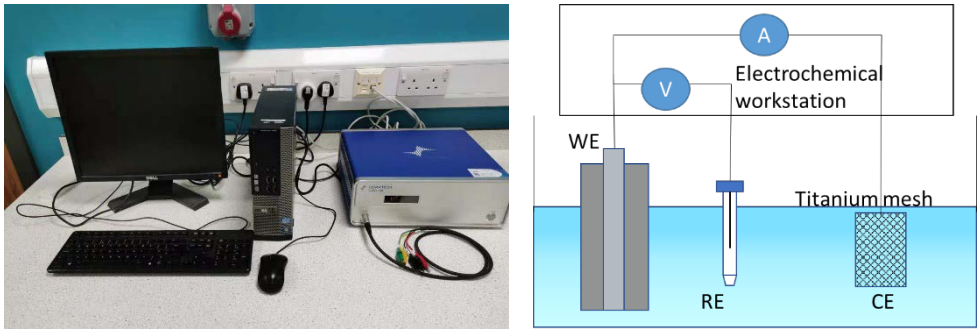

Figure 2. Electrochemical workstation (left) and schematic of the three-electrodes system (right).

The LPR test and Tafel extrapolation method allows to calculate the corrosion rate through Stern-Geary equation (Andrade and Alonso, 1996, Stern and Geaby, 1957):

$$R_P = \left(\frac{\eta}{\Delta i}\right)_{\eta \to 0} \quad (1)$$

$$\mathrm{B} = \frac{\beta_a \beta_c}{2.303(\beta_a + \beta_c)} \quad (2)$$

$$i_{corr} = \frac{\mathrm{B}}{R_p} \quad (3)$$

where η is overpotential ($\eta = E - E_{ocp}$,); R_P is the polarization resistance; B is Tafel constant; β_a and β_c are anodic and cathodic Tafel slope respectively.

The potential dynamic method, with a limited range of overpotentials where $\eta = \pm 20$ mV for LPR test and $\eta = \pm 200$ mV for Tafel extrapolation method was used, with a scan rate 0.167 mV/s.

2.3 Pull-Out Test

The pull-out test was designed to investigate the bond behaviour between reinforced steel and AAC after suffering corrosion. The mixed proportion used for the pull-out test specimens was group 3 from Table 2 because of its high mechanical strength. After curing, the exposed steel bar was twined with copper wire and sealed with epoxy resin. Then, samples were subjected to the cyclic wetting/drying corrosion in chamber to accelerate corrosion before conducting the pull-out test.

According to RC 6 in RILEM technical recommendation for the Testing and Use of Constructions Materials, the bond length for the pull-out specimen should be 5 times the diameter of steel bar. Therefore, the bond length is 60 mm by using Ø12 mm rebar and the concrete specimen size is a block of 150 mm, so a non-bond length of 90 mm was covered by

the acrylic tube, as shown in Figure 3.

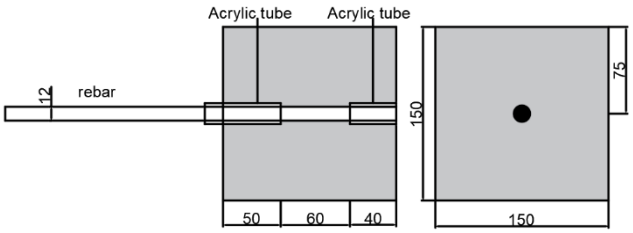

Figure 3. Details of pull-out test specimen (unit: mm).

2.4 Corrosion Environments

In nature, corrosion in reinforced concrete is a very low-rate process that may take up to a few decades to fully corrosion. To obtain data in the short term, artificial corrosion environments including the wetting/drying cycle test and saltwater immersion test were applied to specimens for the purpose of accelerated corrosion. In addition, a control group that tap water immersion was also set.

The cyclic wetting/drying test is performed by using the environmental chamber that controls the parameters (e.g., the temperature) precisely. A wetting/drying cycle contains 2.5 h saltwater fog spray at 25 ℃, 98% RH (relative humidity), and 5 h drying at 50 ℃, 40% RH. The saltwater immersion test was used to simulate the concrete corrosion in seawater, in which 3.5% (by mass) saltwater was used. The saltwater is replaced every week to keep the salt content constant.

3 Results and Discussion

3.1 Pull-Out Test Results

Only two uncorroded specimens were tested due to corrosion time limited, as shown in Figure 4, which the average bond stress was 19 MPa. The ultimate bond stress was calculated through:

$$\tau = \frac{F_{max}}{\pi \phi L} \tag{4}$$

where τ is the ultimate bond stress, ϕ is rebar diameter, L is the bond length and F_{max} is the ultimate pull-out force.

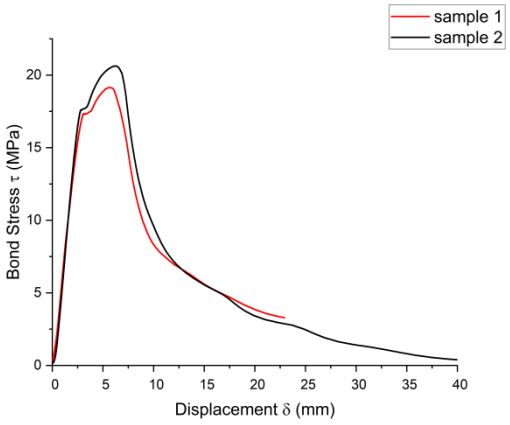

Figure 4. Stress-displacement curves for uncorroded 50% GGBS/50% FA samples.

3.2 Half-cell Potential and Tafel Constant of AAC

Figure 5 presents a comparison of half-cell potential (E_{ocp}) and linear polarization resistance (R_P) values for specimens made with 100% SA (Group 1) and 100% FA (Group 5) in different corrosion environments. Results indicate that both type of specimens exhibits E_{ocp} values as low as -600 mV vs. SCE. The high negative half-cell potential value of 100% SA specimens can be attributed to the presence of sulphides in slag precursors, while the latter (100% FA specimen) is probably due to its porous microstructures (García-Lodeiro et al., 2013) that cause corrosive ions ingress easily.

From Figure 5 b), it can be observed that the 100% FA has the lowest R_p value no matter in what corrosion environment. This is due to the microstructure difference between the two types specimens, with the N-A-S-H (100% FA) exhibiting a more porous microstructure compared to C-A-S-H (100% SA) which has more tortuosity and denser microstructure (Provis et al., 2012). Besides, leaching is a severe issue in alkali-activated materials that it has a detrimental effect on R_p. This is because the high alkalinity of AAC pore solutions cause the alkali ions, which are associated with hydroxyl, to leach out into the external solution due to humidity differences and recrystallization on the concrete surface. This process can cause efflorescence on the concrete surface, and the pH in AAC pore solution could be decreased (Chen and Ye, 2023), leading to reduction in strength and aesthetic loss (Kang and Kwon, 2017). This is supported by the specimens that under cyclic wetting-drying test show the lowest R_p value because cyclic wetting-drying promote the leaching and recrystallization process.

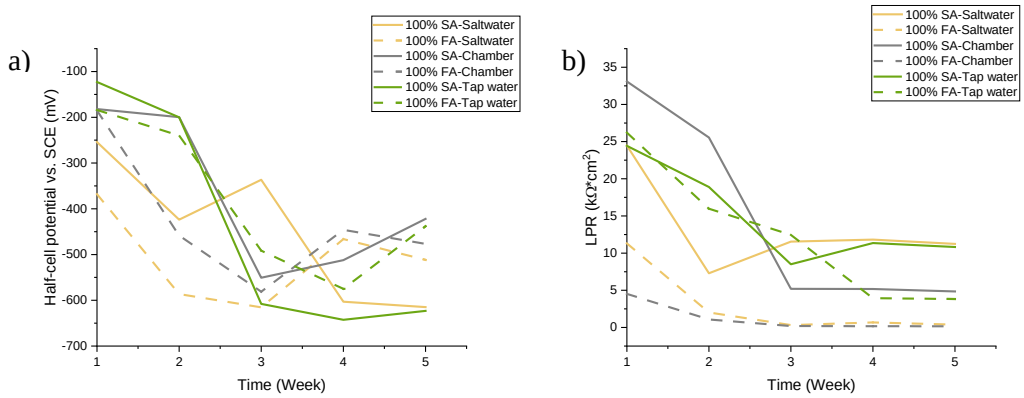

Figure 5. Evolution of Half-cell potential and linear polarization resistance of 100% SA and 100 % FA specimens under three environments.

To evaluate the corrosion current density, which is calculated through Eq. (3), by using the LPR technique, the Tafel extrapolation method was employed to obtain the unknown values that anodic Tafel slope β_a and cathodic Tafel slope β_c. The calculated B values are listed in Table 3. For the OPC concrete, the empirical B value that is used to calculate the corrosion current density is 26 mV for active and 52 mV for passive. However, using these two values will lead to underestimation of the corrosion current density compared with the calculated B value, which is consistent with previous paper (Babaee and Castel, 2016). More details can be found in the author's previous paper (Zhang et al., 2021).

Table 3. The mixed proportion for alkali-activated concrete.

Environments	100% SA	100% FA
Wetting/Drying cycle	38~51 mV	27~37 mV
Saltwater immersion	30~42 mV	22~39 mV
Tap water immersion	31~38 mV	23~32 mV

4 Conclusions

- It can be concluded that the current judging criteria for corrosion possibility from OPC concrete based on ASTM C876 cannot be directly used for reinforced AAC structures because the half-cell potential value of AAC tends to be more negative value easily.
- Tafel constant B tends to increase with the increase of slag content. Besides, the B value is also related to the harshness of the environment, in which the cyclic wetting-drying leads to steel-reinforced ACC damage easier than the other two environments.

References

Ali, M. B., Saidur, R., and Hossain, M. S. (2011). *A review on emission analysis in cement industries*. Renewable and Sustainable Energy Reviews, 15(5), 2252-2261.

Andrade, C., and Alonso, C. (1996). *Corrosion rate monitoring in the laboratory and on-site*. Construction and Building Materials, 10(5), 315-328.

Babaee, M., and Castel, A. (2016). *Chloride-induced corrosion of reinforcement in low-calcium fly ash-based geopolymer concrete*. Cement and Concrete Research, 88, 96-107.

Bouteiller, V., Cremona, C., Baroghel-Bouny, V., and Maloula, A. (2012). *Corrosion initiation of reinforced*

concretes based on Portland or GGBS cements: Chloride contents and electrochemical characterizations versus time. Cement and Concrete Research, 42(11), 1456-1467.

Castel, A., and Foster, S. J. (2015). *Bond strength between blended slag and Class F fly ash geopolymer concrete with steel reinforcement*. Cement and Concrete Research, 72, 48-53.

Chen, Z., and Ye, H. (2023). *Understanding the impact of main seawater ions and leaching on the chloride transport in alkali-activated slag and Portland cement*. Cement and Concrete Research, 164, 107063.

García-Lodeiro, I., Fernández-Jiménez, A., and Palomo, A. (2013). *Variation in hybrid cements over time. Alkaline activation of fly ash–portland cement blends.* Cement and concrete research, 52, 112-122.

Ismail, I., Bernal, S. A., Provis, J. L., San Nicolas, R., Hamdan, S., and van Deventer, J. S. (2014). *Modification of phase evolution in alkali-activated blast furnace slag by the incorporation of fly ash*. Cement and Concrete Composites, 45, 125-135.

Kupwade-Patil, K., and Allouche, E. N. (2013). *Examination of Chloride-Induced Corrosion in Reinforced Geopolymer Concretes.* Journal of Materials in Civil Engineering, 25(10), 1465-1476.

Provis, J. L., Myers, R. J., White, C. E., Rose, V., and van Deventer, J. S. J. (2012). *X-ray microtomography shows pore structure and tortuosity in alkali-activated binders*. Cement and Concrete Research, 42(6), 855-864.

Sarker, P. K. (2011). *Bond strength of reinforcing steel embedded in fly ash-based geopolymer concrete*. Materials and Structures, 44(5), 1021-1030.

Shi, J. J., Ming, J., and Sun, W. (2018). *Electrochemical behaviour of a novel alloy steel in alkali-activated slag mortars*. Cement and Concrete Composites, 92, 110-124.

Stern, M., and Geaby, A. L. (1957). *Electrochemical Polarization: I. A Theoretical Analysis of the Shape of Polarization Curves*. Journal of the Electrochemical Society, 104(1), 56.

Zhang, F., Xi, X., and Yang, S. (2021). *Research Progress in Corrosion Mechanism of Reinforced Alkali-Activated Concrete Structures*. Corrosion and Materials Degradation, 2(4), 641-656.